Chapter 29
Reliability Considerations in the Seismic Capacity Design Requirements for Force-Controlled Components

Victor K. Victorsson[a], Jack W. Baker[b] and Gregory G. Deierlein[b]

Abstract This paper describes factors to consider in developing a methodology to establish capacity-design criteria for force-controlled elements in seismic force resisting systems. The focus is on capacity-designed connections in steel concentrically braced frames, but the concepts can be generally applied to other structural components and systems. The proposed methodology is an adaptation of the load and resistance factor design (LRFD) methodology, where the load effects are defined by the force demands from yielding components of the system. Demand and capacity factors (analogous to load and resistance factors) are determined considering the variability in inelastic earthquake demands and component capacities, along with a target reliability. The target reliability is based on a comprehensive collapse risk assessment that is evaluated using nonlinear dynamic analyses and benchmarked to the collapse safety of modern code-conforming buildings.

Keywords: seismic design, capacity design, reliability, steel structures, collapse safety, load and resistance factor design

23.1 Introduction

Most modern building codes employ capacity design principles to help ensure ductile response and energy dissipation capacity in seismic force resisting systems. The design provisions are geared toward restricting significant inelastic deformations to those structural components that are designed to sustain large inelastic deformations. Such elements are often referred to as deformation-controlled components. Other structural components, referred to as force-controlled components, are designed with sufficient strength to remain essentially elastic, even under large earthquake ground motions.

The 2010 AISC *Seismic Provisions* [1] for brace connections, columns and beams in steel Special Concentrically Braced Frames (SCBFs) are one example of where capacity design principles are used to design force-controlled elements. The

[a] Swiss Reinsurance Company Ltd, Switzerland

[b] John A. Blume Earthquake Engineering Center, Dept. of Civil & Environmental Engineering, Stanford University, US

design provisions aim to confine significant inelastic deformation in the braces while the brace connections, columns and beams remain essentially elastic. The design intent is achieved by requiring that the design strengths of brace connections, columns and beams exceed the expected strength of the braces by an appropriate margin, considering the inherent variability in the force demands and component strengths. In concept, the capacity design requirement is given by the following equation:

$$\phi C_n \geq \gamma D_n \tag{1}$$

where C_n is the nominal strength of the force-controlled component, D_n is the nominal force demand, imposed by the yielding component; and γ and ϕ are demand and capacity factors (similar to load and resistance factors), which are determined based on a target reliability for the force-controlled component.

As the primary goal of seismic building code provisions is to ensure that buildings have adequate collapse safety, the safety margins for capacity design should be determined in the context of the overall system safety. Thus, the establishment of capacity design requirements should consider the following questions:

1) What is the likelihood that the imposed force demand will exceed the strength of capacity designed force-controlled components?
2) How does the failure of a capacity designed component impact the collapse safety of the overall structural system?
3) What are the appropriate demand and capacity factors, and γ and ϕ, to ensure that the system meets the target collapse safety for new buildings.

In this paper, methods to address these questions will be illustrated through an application to evaluate design requirements for braced connections in a six-story SCBF building. The example is based on a more comprehensive study ofthe reliability of capacity-designed components by Victorsson et al. [2].

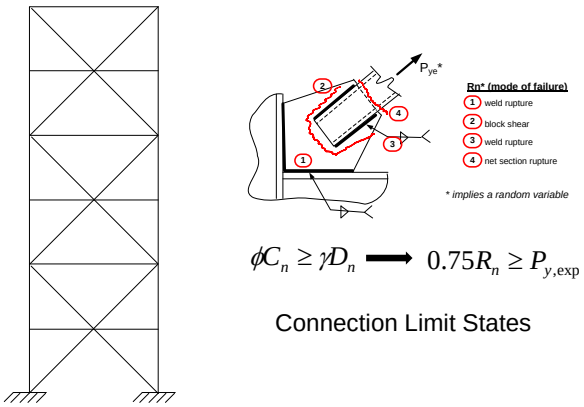

Fig. 23.1 Force-controlled limit states design for brace connections in steel special concentrically braced frame (SCBF)

23.2 Seismic Collapse Safety of Modern Buildings

The FEMA P695 report on *Quantification of Building Seismic Performance Factors* [3] provides a framework to evaluate the collapse probability of building seismic systems. The framework provides a basis to establish minimum seismic design forces and related design requirements for seismic systems that helps ensure consistent collapse safety among the alternative building systems and materials permitted by modern building codes. The FEMA P695 framework employs nonlinear dynamic analyses to evaluate collapse probabilities, taking into account (1) variability in earthquake ground motions, (2) uncertainties in the design, quality assurance and nonlinear analysis, and (3) incomplete knowledge of the structural behavior.

The FEMA P695 framework assesses the reliability of structural systems by nonlinear dynamic analysis of structural archetype models, which are designed to generally represent the characteristics of the building system designation in the building code (e.g., steel SCBF). FEMA P695 specifies a set of 22 ground motion pairs, which are applied to the nonlinear analysis models with increasing intensity, i.e. using an Incremental Dynamic Analysis (IDA), until structural collapse is detected. The analysis data are used to determine the median ground motion collapse intensity, from which a collapse fragility curve is developed assuming a lognormal cumulative distribution function with a specified dispersion (logarithmic standard deviation) and an adjustment to account for ground motion spectral shape effects. The resulting collapse fragility curve (see Fig. 23.2) relates the ground motion intensity, described in terms of spectral acceleration (*Sa*), to the probability of collapse, i.e. $P(Collapse \mid Sa)$. Based on judgment informed by benchmark studies of several code-conforming systems, FEMA P695 specifies a maximum tolerable collapse risk of 10% under *maximum considered earthquake* (MCE) ground motion intensities, i.e., $P(Collapse \mid Sa_{MCE}) \leq 10\%$.

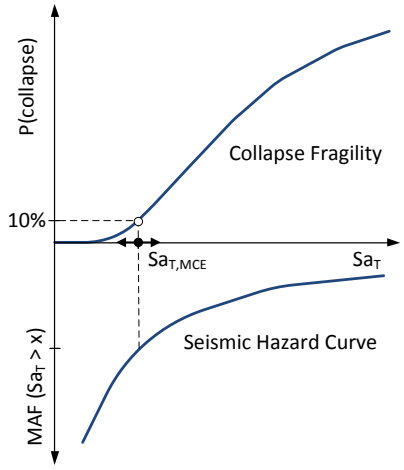

Fig. 23.2 Integration of collapse fragility and seismic hazard curves

Building on the collapse fragilities defined in FEMA P695, the MCE seismic design maps for the United States have recently been revised to provide more consistent collapse risk safety throughout various regions of the United States [4]. These new MCE design maps are predicated on achieving a maximum uniform risk of collapse less than a 1% chance of exceedence in 50 years. This is in contrast to the prior definition of MCE maps, which were associated with ground motion intensities that had a 2% chance of exceedence in 50 years. This recalibration of the MCE maps represents a change from the previous uniform-hazard ground motion intensity to uniform-risk ground motion intensity. As illustrated in Fig. 23.2, the new MCE design map intensities are obtained by integrating site ground motion hazards with a generic collapse fragility curve with a lognormal distribution and an assumed dispersion of 0.6, which is reasoned to be a conservative estimate based on FEMA P695 procedures. With the fixed dispersion of 0.6, the lognormal collapse capacity curve can be fully described by the assumed 10% probability of collapse at the MCE intensity (as specified in the FEMA P695 procedures). Thus, given the default collapse fragility and the ground motion hazard curve for a specific site, the MCE intensity is then calculated for each map location, such that the integration of the two yields the target collapse risk of 1% in 50 years, i.e., $P(Collapse)_{50yrs} \leq 1\%$. The resulting uniform risk MCE design maps have been adopted into the 2010 edition of the ASCE 7 [5] standard for seismic design in the United States. These developments are significant as they establish procedures and target collapse safety risk that provide the basis for establishing seismic design guidelines for new buildings.

23.3 Probability of Demand exceeding Capacity of Force-Controlled Components

The nonlinear dynamic analyses used to establish the median collapse capacity in the FEMA P695 and similar procedures are typically performed using models that are calibrated to the expected values (central values) of the structural response parameters. As such, these collapse analyses do not directly account for the risk of failure in force-controlled components, since the expected properties of the force-controlled components are, by design, larger than the expected demands from yielding elements. Therefore, additional measures are needed to evaluate the failure risk in force-controlled components and how it may impact the collapse risk to the overall structural system. Assuming that the risk of collapse can be evaluated separately for the overall system, where force-controlled components are assumed to remain intact, $P(Coll_{D\leq C})_{50yrs}$, and the additional risk of collapse due to failure of force-controlled components, $P(Coll_{D>C})_{50yrs}$, then the total collapse risk is simply the sum of these two, where the probability is calculated based on a mean annual frequency over a 50-year time horizon:

$$P(Collapse)_{50yrs} = P(Coll_{D\leq C})_{50yrs} + P(Coll_{D>C})_{50yrs} \quad (2)$$

The first term in Eq. 2, $P(Coll_{D\leq C})_{50yrs}$, can be determined by procedures similar to those of FEMA P695 where the capacity-designed components are assumed to remain intact. The focus of this study is on the second term, corresponding to collapse risk due to failure of the force-controlled components, $P(Coll_{D>C})_{50yrs}$.

Shown in Fig. 23.3 are nonlinear analysis results for a six-story SCBF that has been designed using the ASCE 7 and AISC Seismic Provisions for an MCE spectral intensity of Sa(T1) equal to 1.1g and a system response factor of R equal to 6. The nonlinear analyses incorporate the effects of brace yielding, buckling and fracture, degrading flexural hinging in the beams and columns, and large deformation (P-D) effects. As such, the analyses do a reasonably good job at capturing nonlinear behavior up to the onset of collapse. Figures 23.3a and 23.3b show results of an incremental dynamic analysis and the resulting collapse fragility calculated following the FEMA P695 procedures, where the risk of collapse under MCE ground motion intensity is about 10%. Figures 23.3c and 23.3d show how the maximum brace forces develop under increasing ground motion, where the brace force is normalized by the expected tension strength of the braces. Points to note from these figures are (1) that the brace forces increase very rapidly and saturate at their maximum values at ground motion intensities significantly below the MCE intensities, and (2) in contrast to the large variability in drift response (Fig. 23.3a) the variability of the maximum brace forces (Fig. 23.3c) is well constrained about the expected brace yield strength.

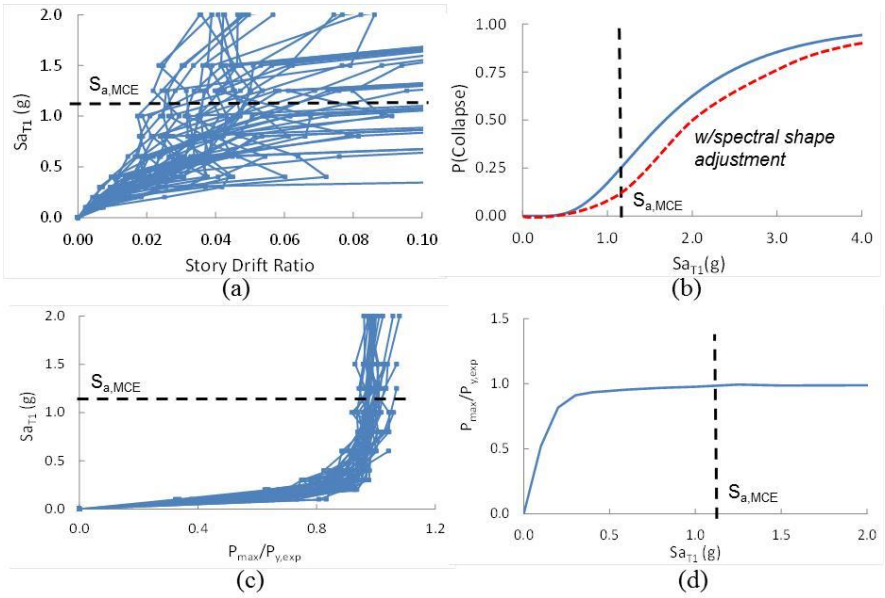

Fig. 23.3 Nonlinear analysis results of 6-story SCBF (a) incremental dynamic analysis – spectral ground motion intensity versus story drift ratio, (b) collapse fragility curve assuming brace connections intact, i.e., D<C, (c) normalized brace force demands versus ground motion spectral intensity, (d) median normalized brace force demands versus ground motion spectral intensity.

Referring to Fig. 23.3a and 23.3b, the variable brace force demand (D) can be compared to the brace connection capacity (C) to determine the probability that the demand exceeds the capacity at variable ground motion intensities. As indicated, the failure probability can be controlled by the ratio of demand to capacity factors, γ and ϕ. Much like the brace force demand, the conditional probability of connection failure, $P(D>C)|Sa$, plotted in Fig. 23.3c, increases rapidly and saturates well below the MCE ground motion intensity. Thus, when integrated with the seismic hazard curve (Fig. 23.2), the early rise in $P(D>C)|Sa$ would lead to rather frequent expectations of connection failures. The steep increase in the plot of Fig. 23.3c further suggests that the calculations could be simplied by approximating the curve with a step function, which increases from zero to the expected $P(D>C)$ at a ground motion intensity corresponding to the point of significant yielding, $Sa_{,yield}$, in the structure. This approximation can simplify calculations for the risk occurance of connection failure, i.e., the mean annual frequency $MAF(D>C)$, by replacing the integration to a simple product of $P(D>C)|Sa > Sa_{,yield}$ and the mean annual frequency $MAF(Sa>Sa_{yield})$, which can be obtained from the ground motion seismic hazard curve. Mathematically, this is as follows:

$$MAF(D > C) \cong P(D > C \,|\, Sa > Sa_{yield}) * MAF\left(Sa > Sa_{yield}\right) \tag{3}$$

In this example, $Sa_{,yield}$ is equal to about 0.25g (about one quarter of the MCE intensity) and has a MAF of exceedence of 0.01/yr for the chosen building site. When multiplied by the risk of connection failure (D>C, assuming a 0.09 failure probability for $Sa>Sa_{,yield}$) the result is about a 4.5% chance of connection failure in 50 years. This 4.5% probability of connection failure is over four times the maximum target risk of building collapse of 1% in 50 years.

23.4 Collapse due to Failure of Force-Controlled Components

As shown in Fig. 23.4d, if one conservatively assumes that brace connection failure triggers frame collapse, then the probability of brace connection failure (Fig. 23.4c) would simply add directly to the probability of system collapse, obtained from the incremental dynamic analyses of the overall system (Figs. 23.3a and b). If judged by the change in collapse probability at the MCE intensity, the risk of connection failure would increase the probability of collapse, $P(Collapse)_{MCE}$, by about 1.8 times, from the original collapse probability of about 12% (w/o connection failure) to 21% (with connection failure). However, when integrated with the ground motion hazard curve to determine the annual rate of failure (e.g., as illustrated in Fig. 23.2), the addition of the connection failure probability to the collapse fragility curve (Fig. 23.4d) has a much more dramatic effect on the collapse risk. This occurs because of the rapid increase in probability of connection failure at the low and frequent ground motion intensities. For example, when integrated with a hazard curve for the high seismic region of coastal California, the dashed fragility curve of Fig. 23.4d that includes connection failure would result in a

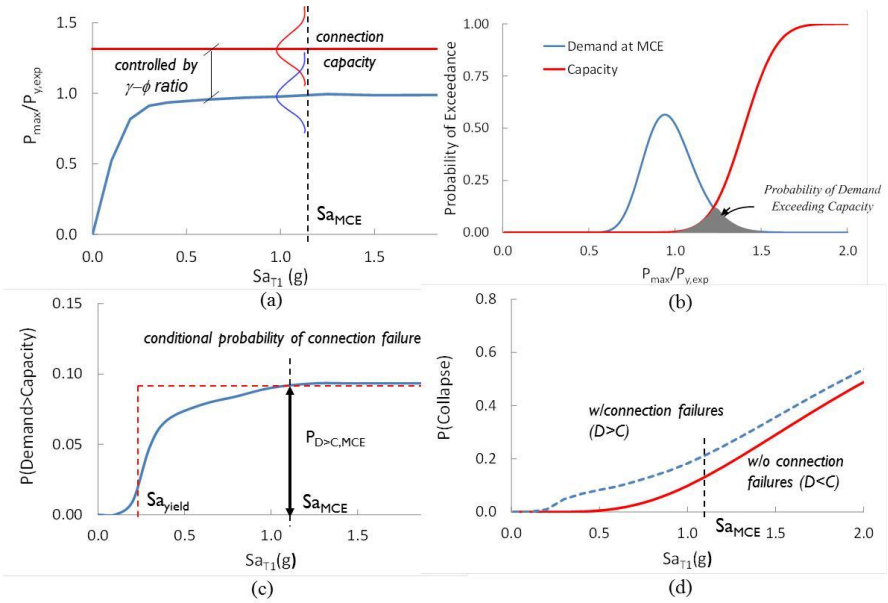

Fig. 23.4 Connection failure data for six-story SCBF: a) normalized brace force b) Elevation of frame, c) Maximum brace forces, P_{max}, recorded in each analysis normalized by expected yield strength, $P_{y,exp}$, d) Probability of connection failure vs. spectral acceleration for a given connection capacity and dispersion.

P(Collapse)$_{50years}$ of 5.5%, which is over six times larger than the than the 0.9% probability calculated for the base fragility without connection failures. This example demonstrates how it can be misleading to evaluate collapse risk only at the MCE intensity as compared to integrating the full range of intensities with the seismic hazard curve. This has obvious implications on current engineering practice, where it is not uncommon to evaluate force-controlled limit states only at MCE level intensities, which can give misleading impressions as to the risk of failure.

While the simple addition of connection failure probability to the overall collapse probability is a logical first approximation, especially for systems with low redundancy such as the braced frame considered here, closer analysis shows that this can be a very conservative assumption. To more carefully assess how connection failures impact the overall frame stability, we conducted additional nonlinear response history analyses where connection failure was simulated directly. Since the connection failure criteria are uncertain, the analyses were conducted using a Monte Carlo type assessment where the brace connection strengths were assumed as uncorrelated random variables.

The Monte Carlo nonlinear analyses are initially performed with brace connection fracture excluded, and then the probability of brace demand exceeding the connection capacity is calculated for the non-collapsed cases. With an assumed median connection capacity of 1.35 times the median brace yield strength and dis-

persion of 0.15, the probability of demand exceeding capacity is calculated using the component reliability concepts described in the previous section. The connection strengths of the Monte Carlo realization are then incorporated in the model and the dynamic analyses are re-run for the cases where the connection capacity is less than the brace demand. The number of additional collapses due to connection failure is then incorporated into the collapse fragility curve.

Figure 23.5a demonstrates that the added probability of collapse due to connection fractures it not constant and initially increases as the ground motion intensity Sa_{T1} increases. In other words, $P(Coll_{D>C})|D>C)$ varies with the ground motion intensity, Sa_{T1}. No new collapses are recorded at Sa_{T1} = 0.40g, suggesting that at this ground motion intensity, the frame is robust enough that it can survive even if connections fracture. As the ground motion intensity increases, the frame's inherent collapse resistance decreases and $P(Coll_{D>C})|D>C, Sa)$ increases. These results tend to agree with conclusions from Luco and Cornell [6] on the effects of brittle connection fractures in steel special moment resisting frames, i.e. that the effect of connection fractures is less pronounced at lower ground motion intensities than at higher ones. These results greatly reduce the influence of brace connections on the system reliability as even if braces are likely to fracture at low spectral accelerations, i.e. close to $Sa_{y,exp}$, the probability of frame collapse is low.

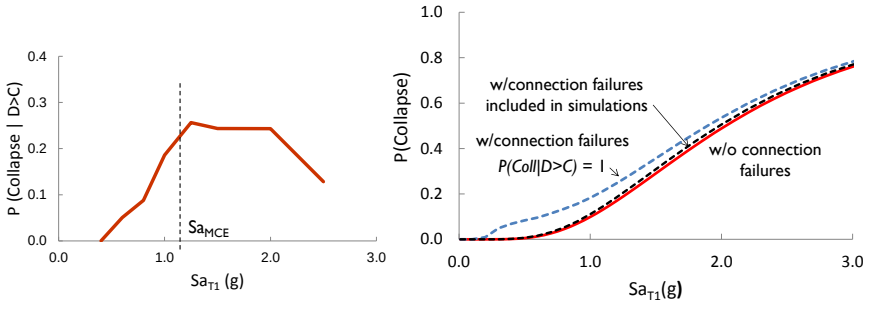

(a) (b)

Fig. 23.5 Collapse probabilities for six-story SCBF: a) change in collapse probability conditioned on connection failure b) collapse fragility curves with and without connection failures.

Using the plot of the probability of collapse conditioned on connection failure for non-collapsed frames, $P(Coll_{D>C})|D>C)$, from Fig. 23.5a, combined with the previous data on the probability of connection failure, $P(D>C)|Sa$, from Fig. 23.4c, the total collapse fragility curve is calculated as shown in Fig. 23.5b. The lowest curve (solid red line) and the upper curve (blue dashed line) are the two cases shown previously (Fig. 23.4d) without and with connection failures; and the middle curve (black dashed line, close to the solid red line) represents the case with connection failures and including the conditional probability from Fig. 23.5a. As indicated, by considering the data on conditional collapse probabilities, the resulting collapse fragility indicates that connection failure has a very modest influence on the final collapse fragility. When the three fragility curves from Fig. 23.5b are integrated with the seismic hazard curve, the resulting collapse probabilities, $P(Collapse)_{50yrs}$, are 0.85%, 0.90% and 5.50%, respectively. Thus, the addi-

tional probability of collapse due to connection fractures is only 0.05% in 50 years, which is dramatically less than the value calculated when the conditional collapse probability (Fig. 23.5a) is ignored. It is important to note that the data in Fig. 23.5a are based on analyses where the variability in connection strength is assumed to be uncorrelated. Correlation between uncertainties in connection strengths will generally worsen the performance, though not to the extent as when connection failure is assumed to be synonymous with collapse.

23.5 Reliability-Based Method to Determine Capacity-Design Factors for Force-Controlled Components

The analyses presented above demonstrate how the risk of failure of force-controlled components is related to the overall risk of collapse to the structure. Ultimately, the target probability of failure (or reliability index) of the force controlled components depend on the following factors:

$P(D > C)|Sa>Sa_{,yield}$): the probability that the force demand D imposed by yielding components will exceed the capacity C, conditioned on the structure having experienced ground motions to initiate yielding.

MAF ($Sa>Sa_{,yield}$): the mean annual frequency that the structure will experiences ground motions that initiate significant yielding in the members that generate forces in the force-controlled components.

$P(Coll_{D>C}|D>C, Sa)$: the probability of collapse caused by failure of force-controlled components. As illustrated in Fig. 23.5a, this probability depends on the ground motion intensity and conditioned on the subset of cases where the structure has not collapsed due to other factors (e.g., sidesway collapse where the force-controlled components are intact).

Target MAF ($Collapse_{D>C}$) or $P(Collapse_{D>C})_{50yr}$: the maximum permissible mean annual frequency of structural collapse, due to failure of the force controlled components. As described per Eq. 2, this target probability is constrained by the target limit on structural collapse from all causes, assumed to be on the order of 1% in 50 years, per Luco et al. [4], and the probability of collapse due to factors other than failure of the force-controlled components, which is assumed to be the main contributor to collapse.

Of these four probabilities, the first, *$P(D > C)|Sa>Sa_{,yield}$)*, can be described in a design-sense in terms of an LRFD-like formulation [7,8] in which the reliability index, β, can be calculated as follows:

$$\beta = \frac{\ln\left(\frac{D_n}{D_m}\frac{C_m}{C_n}\frac{\gamma}{\phi}\right)}{\sqrt{V_C^2 + V_D^2}} \tag{4}$$

where D_n and D_m are the nominal and median force demands, C_n and C_m are the nominal and median component capacities, V_D and V_C are variances in the force demands and capacities, γ and ϕ are the demand and capacity factors, and β is the resulting reliability index. Assuming that the force demands and capacities can be described by lognormal distributions, β can be related to the probability of failure (i.e., that $D>C$, conditioned on $S_a > S_{a,yield}$) as shown in Fig. 23.6. In the case of brace connections in steel SCBFs, the connection capacity terms (C_n, C_m and V_C) are the same as those assumed in the standard *AISC Specification* [8] requirements, the nominal demand D_n is the expected yield strength of the brace, $P_{y,exp}$, and the median demand and variability in demand (D_m and V_D) can be developed through nonlinear analysis of SCBFs (e.g., Fig. 23.3) and brace tests. Given this information to characterize the demands and capacities, once a target reliability index is known, then the γ and ϕ factors can be used to adjust the probability of failure of the force-controlled components (e.g., $P(D > C)|Sa>Sa_{,yield}$), as shown in Fig. 23.4.

Reliability Index β	Probability of Failure
0.0	0.5
0.5	0.31
1.0	0.16
1.5	0.07
2.0	0.02
2.5	0.006
3.0	0.001
3.5	0.0002
4.0	0.00003
4.5	0.000003
5.0	0.0000003

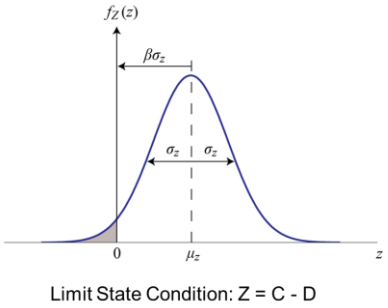

Fig. 23.6 Collapse probabilities for six-story SCBF: a) change in collapse probability conditioned on connection failure b) collapse fragility curves with and without connection failures.

The main challenge in the reliability assessment is to determine the target reliability index, β, which is equivalent to the establishing target failure probability $P(D > C)|Sa>Sa_{,yield}$. The appropriate target reliability (component failure probability) depends on the other three components of the analysis, i.e., $MAF(Sa>Sa_{,yield})$, $P(Coll_{D>C}|D>C, Sa)$, and $P(Collapse_{D>C})_{50yr}$. The first of these, $MAF(Sa>Sa_{,yield})$, depends to a large extent on the seismic response factor that is used to define the required strength (e.g., the R-factor in United States practice), which is based on the inelastic deformation characteristics of the system. The second, $P(Coll_{D>C}|D>C, Sa)$, depends on the dynamic response characteristics, redundancy of the system, and the effect that failures of the force-controlled components have on the overall system behavior. The final term, $P(Collapse_{D>C})_{50yr}$, should probably be limited to about 0.1% to 0.2% in 50 years (MAF of 0.00002 to 0.00004/year), assuming that the total $P(Collapse)_{50yr}$ is limited to 1% in 50 years and that only a small portion (< 10%) of this should be attributed to failure of the force-controlled components.

In studies of SCBFs of the type described in this paper, the authors found that reliability indices, β, on the order of 2.5 provided acceptable performance. From Fig. 23.6, this β corresponds to a $P(D > C)|Sa>Sa_{,yield})$ of about 0.006, or 0.6%. When combined using Eq. 4 with available statistical data on force demands and capacities (D_n, D_m, C_n, C_m, V_D and V_C), this β of 2.5 implies that the demand and capacity factors of γ=1.0 and ϕ=0.75, as specified for bracing connection components by the current AISC Provisions [1,8], are slightly conservative. Of course, while the underlying methodology outlined in this paper can be generally applied, the specific numerical results depend on data and assumptions that are specific to the SCBFs considered in this study.

23.6 Concluding Remarks

While the basic principle of capacity-design is straightforward, its implementation is complicated by uncertainties in the force demands and capacities, which introduce ambiguities as to how strong to make the force-controlled components. The calculation of appropriate demand and capacity factors for force-controlled components requires consideration of the overall system reliability, in order to maintain a reasonable balance between the achieving the idealized inelastic mechanism (as envisioned by capacity-design approach) and practical and economic limits on design. The proposed reliability-based methodology to establish capacity design requirements incorporates the main factors believed to influence the reliability of force-controlled components. While further work is needed to quantify the constituent components of the reliability assessment, the proposed methodology is intended to provide a framework that will enable the calculation of risk consistent capacity-designed components for structural components and systems.

23.7 Acknowledgments

The authors would acknowledge the contributions of the late Professors Allin Cornell and Helmut Krawinkler to this research. Both of these individuals were involved in the early stages of this project and generously shared their knowledge and expertise. The authors would also acknowledge the advice and encouragement of Tom Schlafly and others on the specification committee of the American Institute of Steel Construction, who reviewed this project. The financial support of the American Institute of Steel Construction, the National Science Foundation (CMMI-1031722, Program Director M.P. Singh), and the Blume Earthquake Engineering Center at Stanford University is also acknowledged. The findings and conclusions made in this paper are those of the authors and do not necessarily reflect the views of the sponsors.

References

1. American Institute of Steel Construction Inc. (2010). *Seismic Provisions for Structural Steel Buildings*. AISC, Chicago, IL.
2. Victorsson, V.K., Deierlein, G.G., Baker, J.W., Krawinkler, H. (2012). *The Reliability of Capacity-Designed Components in Seismic Resistant Systems, J.A. Blume Technical Report 177*, Stanford University, Stanford, CA.
3. FEMA P695 (2009). *Quantification of Building Seismic Performance Factors.* Federal Emergency Management Agency.
4. Luco, N., Ellingwood, B.R., Hamburger, R.O., Hooper, J.D., Kimball, J.K., Kircher, C.A., (2007). "Risk-Targeted versus Current Seismic Design Maps for the Conterminous United States" *Proceedings SEAOC 2007 Annual Conference*, 13 pgs.
5. American Society of Civil Engineers (2010). *ASCE-7-10: Minimum Design Loads for Buildings and Other Structures*, Reston, VA.
6. Luco, N. and Cornell, C.A. (2000) "Effects of connection fractures on SMRF seismic drift demands". *ASCE Jl. of Structural Engrg.,* 126(1), pp. 127-136.
7. Ravindra, M.K., Galambos, T.V. (1978) "Load and resistance factor design for steel." *Jl. of the Structural Div.*, ASCE 1978; 104(STD9): pp. 1337-1353.
8. American Institute of Steel Construction Inc. (2010) *Specification for Structural Steel Buildings*, AISC, Chicago, IL.